Design and Development of Biosensors Based on Nano Tube Tunnel Field Effect Transistor

Masoud B M Alsalman*, Msaid Alsaleh**
*(Department of Electrical Engineering, Shuwaikh Institute, PAAET, Kuwait.
Email: mb.alsalman@paaet.edu.kw)
** (Department of Electrical Engineering, Shuwaikh Institute, PAAET, Kuwait.
Email: maa.alsaleh@paaet.edu.kw)

ABSTRACT
Tunnel Field Effect Transistor (TFET) is gaining recognition and provide solution for Integrated Circuit (IC) design with low power. This is due to TFET's carrier transportation scheme, which utilizes inter-band tunneling of carriers, and its fabrication similarity to MOSFET. TFET presents itself as a widely adopted device structure that can overcome the limitations of MOSFETs. However, TFETs suffer from poor DC and Radio Frequency (RF) performance, mainly due to minority carrier transport and physical doping, which forms an abrupt junction in nanoscale devices due to RDFs. The junction-less device structure presents a viable solution to these issues without sacrificing DC parameters, even at high-frequency. Furthermore, the nanotube structure of TFET effectively reduces the Subthreshold Swing (SS) and leakage current due to better controllability of channel. The gate-all-around structure of nanotube TFET improves the surface potential distribution over the channel region, not only enhancing the DC characteristics of TFET but also improving the high-frequency parameters. The core gate Nano Tube (NT)-TFET is a promising device structure for exploring its application in the field of biomedical science as a biosensor. The proposed core gate nanotube structure provides a larger surface area for immobilizing biomolecules in the cavity, thus improving sensitivity analysis. This work proposes the utility of a novel core gate NT-TFET as a biosensor for detecting label-free biomolecules and DNAs. In this design, the detection capability of biosensor is improved, and the detection processes are investigated by high-frequency parameters of the proposed twin cavity dual metal NT-TFET biosensor. This study demonstrates the sensitivity analysis of biosensor based on transit time and device efficiency, which are two critical high-frequency parameters. This approach results in a biosensor with a lower annealing budget, making it more cost-effective and with comparatively higher sensitivity.

Keywords **-** Nanotube, Tunnel Field Effect Transistor, Charge Plasma, Biosensor, Sensitivity, Gate controllability.

I. INTRODUCTION

Advancements in modern electronic devices have contributed so much for making human life easier in many ways. Moreover, ingenious ways have been found by scientists to execute digital and analog functions using MOSFET circuit designs [1]. Thus, MOSFET has become the desired and preferred device to be fabricated in the semiconductor industry [2]. But downscaling of the feature size of the device also causes various issues such as Short Channel Effects (SCEs) or second-order phenomenon and several sorts of problems came across when the lithography goes below 100 nm technologies. At the industry level generally, full scaling is preferred. This scaling option attempts to maintain the same magnitude of internal electrical fields even after scaling the dimensions (channel length, oxide thickness, channel width, and junction depth), let say by the factor S. For achieving this threshold voltage (Vi) and power supply are also needed to be scaled by the same factor. On the other hand, in constant voltage scaling, dimensions are scaled down by the constant factor. But biasing voltages remain the same, which leads to an increment in the electric field and doping density within the device.

Threshold voltage (V_{th}) variation is the smallest amount of V_{GS} essential to create a conducting path between drain and source region of MOSFET. The voltage at which the device initiates its activation is V_{th}. But due to SC distance, the applied V_{DS} reduces the energy barrier of the MOSFET, without the application of VGS. Hence less V_{th}, is required to move carriers from source to drain. This change in V_{th} is known as V_{th} variation or V_{th} roll-off [3]. Transistors with different channel lengths experiences different values of V_{th}, in the same silicon wafer. This effect results from a reduction in drain region. Since the charge sharing effect is greater between the channel depletion region and S/D depletion area the devices have longer channel

lengths. Dynamic dissipation in power consists of two components, the first is the additional switching power generated by the charging and discharging of load capacitors, and it is dependent on the switching frequency. The second component of power dissipation is caused by current flow when the device's transistor switches from one logic state to another. The dynamic power dissipation is formulated as:

$$P_D = C \times f \times V_{DD}^2 \quad (1)$$

Where, C is capacitance, f is operating frequency and V_{DD} is power supply. The static power dissipation of a CMOS circuit is measured by the leakage current ($I_{leakage}$) through each transistor.

$$P_S = V_{DD} \times I_{leakage} \quad (2)$$

With the downscaling of technology, V_{DD} needs to be reduced to reduce power dissipation. The root cause of the increase in power density is that the V_{DD} required to drive the transistor cannot be increased in proportion to the transistor density. It is because, since the device is reducing the operating voltage, these could not be scaled proportionally. Hence, P_D need to be reduced, which can be done only by reducing the $I_{leakage}$.

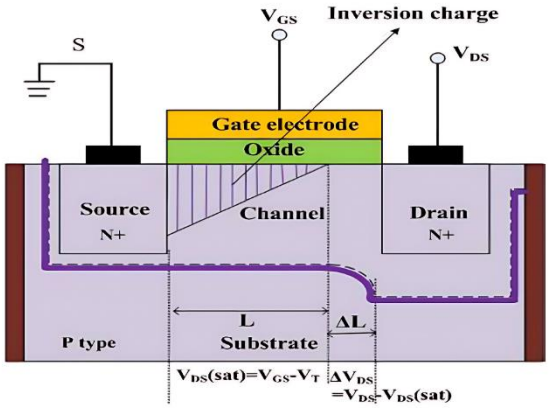

Fig. 1: Cross-section of channel length modulation

With the miniaturization, the technology enters the quantum region where the TFET can be a good candidate as a novel device design that is based on quantum tunnelling carrier transport as compared to conventional thermionic emission. TFET has a lower $I_{leakage}$ subthreshold swing (SS) is outreached, from Boltzmann tail phenomena, so TFETs can significantly reduce $I_{leakage}$ and SS compared to thermionic emission-based devices. Unlike MOSFETs, the SS of a TFET, it has a lower V_{th}, which makes it suitable for switching applications. Apart from these, TFET has a similar fabrication design structure as MOSFET, it is immune to SCEs, and V_{th}, also can be reduced considerably.

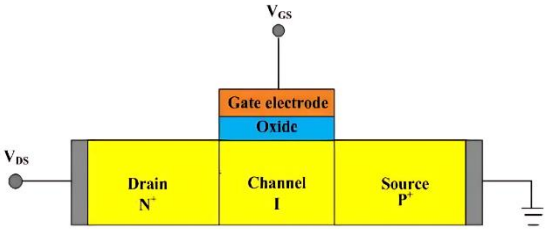

Fig 2: Cross-sectional view of single gate n-type TFET.

Base assembly of TFET is very identical to traditional MOSFET, except the channel is intrinsic or lightly doped and sandwiched between source and drain which resembles a P-I-N diode. The Cross-section of single gate NT-TFET is depicted in Fig. 2. Conventional TFET can work for both (positive & negative) gate voltage. For N-channel TFET positive V_{GS} is needed for normal operation, and negative gate voltage causes ambipolar characteristics; vice versa is applicable for P-channel TFET. The OFF-state of the device when a positive power supply is given to V_{DS} and Vs is not connected to any bias voltage.

Biosensor design can be categorized into three sub-structures that are bio-receptors, transducers, and readers. Examples of target biomolecules are different kinds of bacteria, viruses, proteins, and DNA. Bio receptors can be cavity-type structures with specialized shapes and materials which can stick to the biomolecules; for different types of biomolecules, different receptors can be designed as per the requirement. The transducer converts the physical signal or changes observed by the biosensor due to the presence of biomolecules into electrical parameters, and these electrical parameters are further sent to a complete circuit that is known as a reader. It stores the output of the transducer for future use such as testing and analysis. There are many transducer-based biosensors available i.e., electrochemical biosensors, optical biosensors, and electronic transducer biosensors. In this dissertation, we have studied the electronic transducer-based biosensors, for example, FET-based and TFET-based biosensors. Fig. 3 displays the general structure of biosensor, which signifies three components of the biosensor.

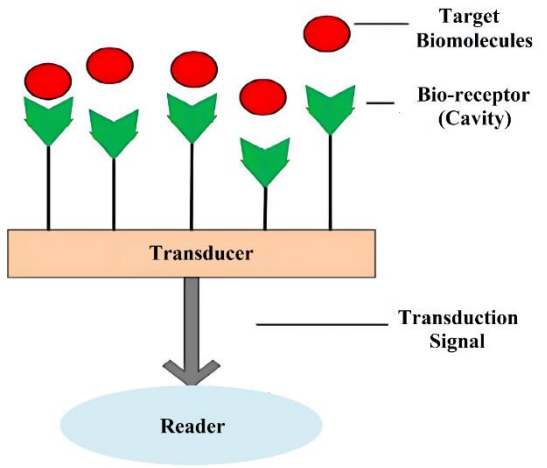

Fig. 3: Generalized block diagram of biosensor

II. RELATED WORKS

In recent technological trends, it is necessary to continuously reduce the dimensions of the device to satisfy Moore's law [4]. The continuing downsizing of the traditional MOSFETSs has demonstrated better performance in various DC/RF parameters [5]. Along with these advantages, downsizing also includes some unnecessary features such as an intolerable increase in $I_{leakage}$. And SCEs [6]. Also, the MOSFET working mechanism (thermionic emission) has a roadblock for the reduction of Vg, switching speed, and SS given by 2.3kT/q where k. T, and q are typical notations. As an alternative to the MOSFET, various new devices appeared. Emerging transistors such as the FinFET have been invented to overcome different performance issues on planar MOSFETs. FinFETs are less affected by SCEs and provide better gate controllability, but the vertical orientation of its fin increases the corner effect, parasitic capacitance that degrades the performance of the IC. In this regard, a currently emerging tunnelling phenomenon has come out as a capable device due to its capability to offer very low IOPR, and SS (60 mV/decade). which has gathered a great attraction compared to MOSFETs. This tunnelling phenomenon allows the downscaling of the bias voltage due to the minimum requirement of switching energy below the 50 nm technology node. Furthermore, the fabrication compatibility of TFETs and suitable characteristics make it a promising substitute for MOSFETs in low-power devices [7]

However, the concept of a tunnelling mechanism had already been invented in 1958. The former P-I-N gated structural design was examined much later in 1978, but the performance of the structure was not valuable. After much research was done, in 1987, a new three-terminal silicon-based tunnelling device with its electrostatic behaviour was investigated for the first time [8]. This demonstrated the output results of the device in a graphical form. After this point, research stated that downscale the dimensions and found that the TFET device is indeed robust against the SCEs. Later, many groups of researchers too came up with some investigations as reported in [9].

TFETs with their unique working principle provide scientists with interest for investigation, and it has become a possible candidate for the next era. A variety of configurations are studied for TFET. and further improvements to the single gate TFET device such as double-gate, heterojunction, and bandgap engineering [10]. Further, the cylindrical nanowire (NW-TFET) showed advanced current driving capability with low SS than planar technology. NT-TFET enhances the TFET performance parameters in various terms. The NT-TFET is having better capability than 2-D or planar devices. In sub-micron technology, doped-TFET (D-TFET) suffers from process variability because of RDFs. Literature also reveals that conventional doped TFETs have high sensitivity towards RDFs as equated with MOSFETs because of the direct influence of tunnelling width. Further, in the next era TFET is discovered in the form of charge plasma. There is much research going on in the field of the biosensors using low-power devices. So much research is going on for the use of low-power device in case of biosensor.

Initially, very well-known techniques have been developed for the detection of DNA biomolecules, but they require a labelling step [11]. Having a labelling step increases the complication of multi-stage investigation, which reduces the efficiency of sampling. In this method, ISFET is employed to detect biomolecules, and are limited in its ability to identify neutral biomolecules. The ISFET detects changes in I_{DS}, conductance, or V_G associated with variations in charged biomolecules. To reduce the effect of this limitation, the DMFET was introduced. The DMFET is capable of efficiently detecting biomolecules, addressing ISFET's shortcomings. Therefore, DMFET-based label-free biosensors attract enormous interest to create ultrasensitive bio-instruments because of their broad sensing ability and considerable impact on the health-diagnostics industry. But FET-based biosensors get complexity in realizing small detection times due to the SS limit (KT/q), which increases the SS of the biosensor.

Due to the increased SS, it lowers sensing ability and longer response time. This time is basically required to sense the various biomolecules in the cavity area. In this regard, a TFET-based biosensor

has been developed as an appropriate candidate. BTBT mechanism in DM-TFET biosensors gives better sensing ability and response time than traditional FET-based biosensors [12]. TFET-based biosensors have gained significant attention in exploring dielectric modulated phenomena, addressing the limitations of MOSFETs. These TFET-based biosensors offer several advantages over MOSFET-based biosensors, including enhanced sensitivity, shorter response time, higher energy efficiency, and reduced leakage current. In [13], the design process of the nanogap cavity in the elevated DM-TFET is illustrated. This cavity is strategically positioned at the biosensor structure where tunnelling occurs. Furthermore, three-dimensional devices such as NW-TFETs have demonstrated improved sensing capabilities in various contexts.

III. MATERIALS AND METHODS

To enable successful prediction of various biomolecules, biosensors need to possess good sensitivity and a well-designed structure. In order to overcome the limitations of 2-D TFET-based biosensors and achieve superior sensing capabilities, efficiency, and low $I_{leakage}$, we propose a novel JL-NT-TFET biosensor in this study [14]. The JL-NT-TFET biosensor incorporates a dual-gate (inner and outer) all-around structure, that function using the charge plasma technique. This unique structure enhances the electronic control of gate over other channel regions and enables scaling towards nano-scale administration. By incorporating gate within the tube, we aim to reduce quantum effects and unwanted charges, thus improving the performance of the biosensor for sensing applications. To enhance efficiency, we introduce two cavities in the inner and outer cylindrical parts of biosensor. These cavities are developed by Cr etching, which allows for thinner layers with uniformity. The combination of Ag and Cr exhibits excellent structural strength and chemical bonding.

The JL-NT-TFET biosensor offers several advantages, such as a smaller SS and a higher I_{ON} with the provision of larger tunnelling area. These advantages lead to suppressed leakage, sharper SS, and an optimized threshold voltage. To provide a comprehensive overview of these benefits, Table 1 presents numerical values that highlight the improvements achieved with the inclusion of the core gate in the biosensor.

Table 1: Properties of JL-NT-TFET

Parameter	**JL-NT-TFET**
I_{ON} (A)	1.11×10^{-6}
I_{OFF} (A)	2.77×10^{-17}
V_{th} (V)	0.318
SS (mV/dec)	19.8
I_{ON}/I_{OFF} ratio	4.01×10^{10}

The dual cavity design of the biosensor plays a crucial role in effectively detecting biomolecules [15]. During detection mechanism, the electric properties of biosensors are sensitive towards biomolecules with diverse dielectric constants (K) within the cavity. Additionally, charged biomolecules, specifically DNA with K=6, are also detected using the biosensor. The sensitivity of the device to various biomolecules is evaluated while the cavities are filled with air (K=1) as a baseline reference. The sensitivity analysis considers various DC performance parameters to assess the detection ability of biosensors [16]. The device is fabricated using N-type junction less silicon technology, employing charged plasma technology for precise control. The nanotube-style biosensor is vertically structured within a wafer. The charge plasma concept allows appropriate Work Function (WF), where the thickness of Si body is lesser than Debye length. In this design, Pt with WF 5.93eV is utilized to create P source. The 3-D schematic structure illustrating with creation of the inner and outer cavities in the JL-NT-TFET biosensor is presented in Fig. 4.

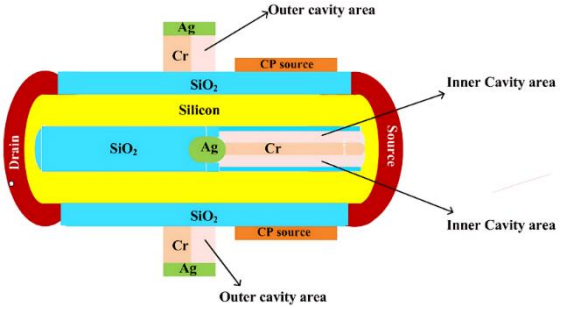

Fig. 4: 3-D structure of JL- NT-TFET Biosensor

Gate and Gate 1 are composed of Cr and Ag with work functions of 4.38eV and 4.46eV, respectively. The use of Ag with a lower work function is intended for low-power devices, enabling the biosensor to activate at a lower applied voltage bias. In biosensor based on JL-NT-TFET, the inner gate made of Ag is shifted towards the source/channel interface, occupying half of the 10 nm channel region. The device features a 10 nm diameter silicon body and an

inner Ag gate. A visual representation of the JL-NT-TFET biosensor's structure is illustrated in Fig. 5.

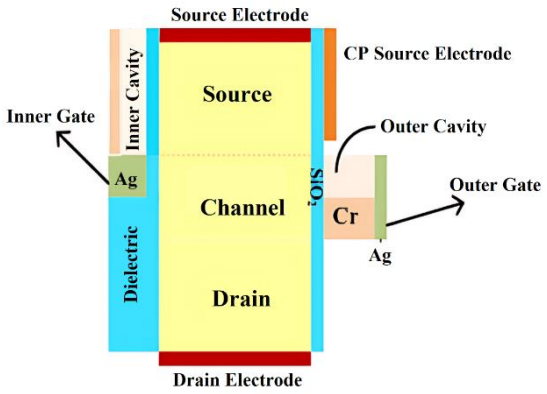

Fig. 5: Vertical 2-D schematic structure of JL- NT-TFET biosensor

The source region of the device is extended to form the outer cavity, projecting from the midpoint of the 10 nm channel region towards the source. Simultaneously, the inner cavity is created within the source region to ensure the uniform distribution of biomolecules. The dimensions of the drain, source, and channel are set at 50 nm, 50 nm, and 22 nm respectively. The outer gate and outer charge plasma electrode lengths are defined as 20 nm and 50 nm, with a 2 nm separation between the outer gate and charge plasma source. To provide protection and stability, the silicon body is coated with a 1 nm thick layer of outer oxide (SiO_2).

IV. RESULTS AND DISCUSSION

To examine the essential properties and underlying physics of the JL-NT-TFET biosensor, we delve into its fundamental characteristics. In this analysis, we focus on the electrostatic behaviour of the biosensor as we vary the dielectric constants associated with different biomolecules.

A. Energy Band Distribution

The effect of biomolecules' K on the capacitive nature of JL-NT-TFET biosensor is evident. As K rises, the device's capacitance increases, subsequently dropping the tunnel barrier at channel/source junction. Notably, protein biomolecule, with a K value of 8, exhibits the smallest tunnelling barrier. To visualize this phenomenon, Fig. 6 depicts the EBD in the ON-state for different K values, all of which are present within the biosensor's cavity.

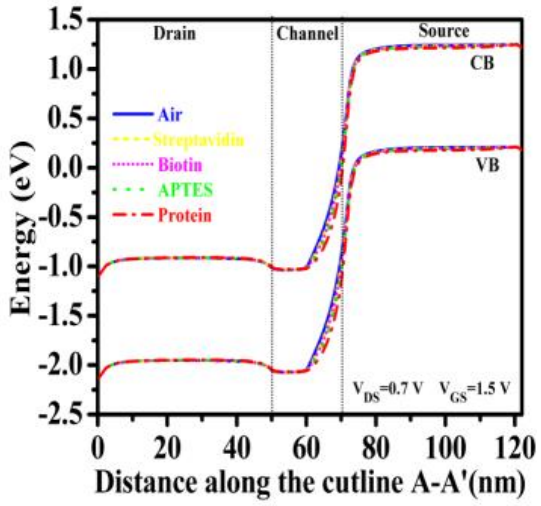

Fig. 6: Energy Band Diagram

B. Electric Field

The reduction in tunnel barrier leads to a further enhancement of field between the channel/source junction. The protein biomolecule, characterized by the highest dielectric constant (K) among the neutral biomolecules, exhibits peak in field. This behaviour is illustrated in Fig. 7, where the electric field shows a similar trend.

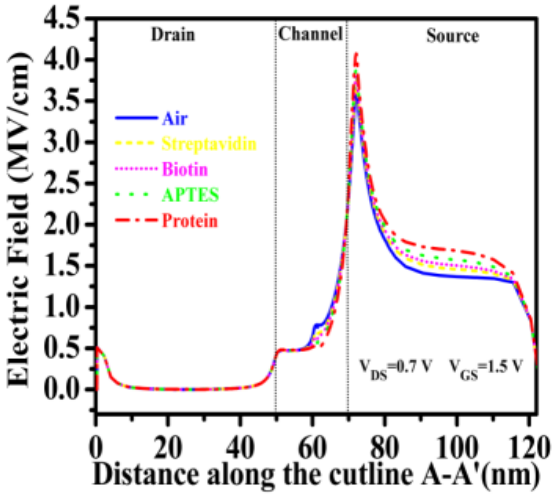

Fig. 7: ON-state electric field for neutral biomolecules.

C. Transfer Characteristics

The I_{DS}-V_{GS} plot of different neutral and charged biomolecules are presented in Fig. 8(a) and Fig. 8(b), respectively. In Fig. 8(a), protein biomolecule exhibits a higher I_{DS} attributed to its higher tunnelling efficiency. This can be attributed to the narrower tunnelling interface. It is observed that I_{DS} rises with the increment in K of neutral biomolecules, indicating a direct relationship between C and K.

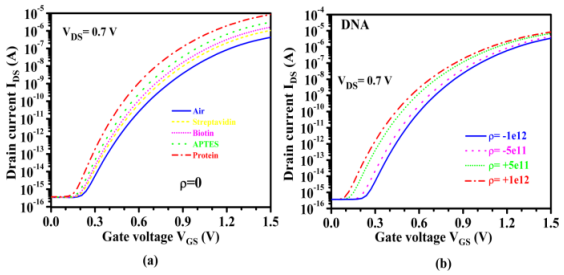

Fig. 8: Transfer characteristics (a) neutral charge (b) charged DNA

In a similar manner, Fig. 8(b) illustrates the transfer (I_{DS}-V_{GS}) characteristics for DNA with varying p. It is observed that I_{DS} increases as the positive charge biomolecule concentration increases, and vice versa. This behaviour can be explained by the fact that positive charge biomolecules enhance the electron population, resulting in increased tunnelling through the barrier. On the other hand, cavity enhancement and hole population lead to a decrease in electron tunnelling for negative charge biomolecules.

D. Sensitivity Analysis

The sensitivity analysis of the biosensor plays a crucial role in detecting and distinguishing variations in target biomolecules compared to the baseline condition. A larger sensitivity value indicates a greater probability of accurately detecting the desired biomolecules. In this study, the biosensor's sensitivity is evaluated through the examination of several DC parameters, including I_{DS}, SS, V_{th} (threshold voltage), and I_{ON}/I_{OFF} ratio sensitivity. These parameters provide insights into the biosensor's ability to detect and quantify changes in electrical characteristics, enhancing its effectiveness for biomolecule detection. The I_{DS} sensitivity is explained as,

$$S_{IDS} = \left| \frac{SS_{IDS(Bio)} - SS_{IDS(Air)}}{SS_{IDS(Air)}} \right| \quad (3)$$

In the context of sensitivity analysis, $SS_{IDS(Bio)}$ and $SS_{IDS(Air)}$ represent the SS_{IDS} with and without biomolecules, respectively. Fig. 9(a) and (b) illustrate I_{DS} sensitivity to V_{GS}, considering various values of K and p (negative and positive). In Fig. 9(a), it is observed that as K of the biomolecule rises, the I_{DS} sensitivity also rises. Notably, streptavidin exhibits lower sensitivity, while protein demonstrates the opposite. In Fig. 9(b), the I_{DS} sensitivity decreases with rise in negative charge density. The highest sensitivity is observed for higher positive charge densities. Furthermore, an interesting finding is that the peak sensitivity is achieved at lower V_{GS}.

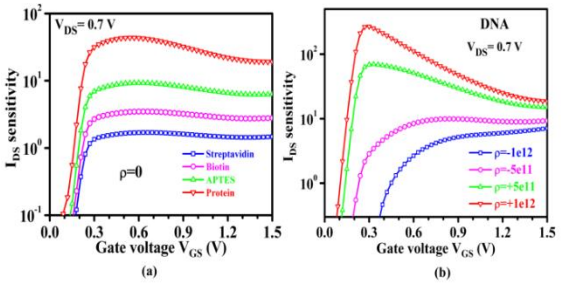

Fig. 9: I_{DS}-V_{GS} Sensitivity graph (c) neutral charge (d) charged

The sensitivity of Subthreshold Swing (SS) is crucial for biosensor efficiency, as it directly influences the speed and efficiency of biomolecule detection. SS sensitivity is computed using Eqn. 4.

$$S_{SS} = \left| \frac{SS_{(Bio)} - SS_{(Air)}}{SS_{(Air)}} \right| \quad (4)$$

The sensitivity of SS is a crucial factor in the performance of the JL-NT-TFET biosensor, indicating its ability to detect biomolecules. In Fig. 10(a-b), the SS sensitivity is demonstrated. Lower SS value implies a higher potential of detection and improved response. Fig. 10(a) reveals a decrease in SS as the K of the biomolecules increases, with protein exhibiting the lowest SS. Similarly, in Fig. 10(b), for charge biomolecules (DNA), the SS of the biosensor increases with respect to charge density. This demonstrates that SS sensitivity of biosensor is influenced by the charge density of the biomolecules, with higher sensitivity observed for higher charge densities.

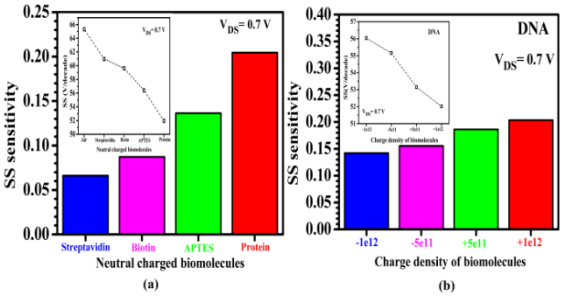

Fig. 10: SS sensitivity graph (a) neutral charge (b) charged (DNA)

V_{th} can be determined by utilizing constant current scheme, where V corresponding to I_{DS} of $1x10^{-7}$A is measured and computed as V_{th}. The V_{th} sensitivity constraint is calculated as:

$$\Delta V_{th} = \left| \Delta V_{th(Air)} - \Delta V_{th(Bio)} \right| \quad (5)$$

In the given equation, $V_{th(Air)}$ and $V_{th(Bio)}$ characterize V_{th} when the biosensor is occupied by air and biomolecules, correspondingly. Moreover, ΔV_{th} defines a shift in V_{th} during biomolecule identification compared to the air-filled state. In Fig. 11(a), comparative V_{th} is depicted, showing that higher the value of K, the V_{th} decreases. Consequently, the I_{DS} reaches $1x10^{-7}$A at an earlier stage compared to the air-filled state. The sensitivity of V_{th} is evaluated using Eqn. (3), and it is observed that protein (K=8) exhibits higher sensitivity. Similarly, in Fig. 11(b) large value of V_{th} is observed for more negative p of DNA, while a lower value of V_{th} is observed. This indicates that V_{th} sensitivity increases with charge shifts.

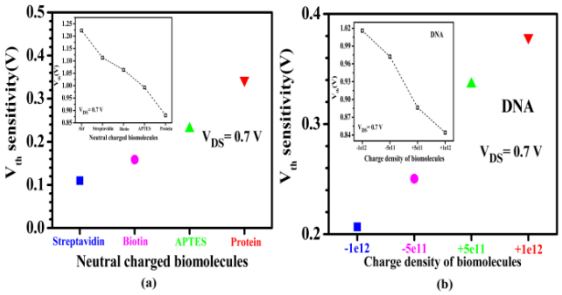

Fig. 11: V_{th} sensitivity graph (a) neutral charge (b) charged (DNA)

I_{DS} sensitivity is obtained using Eqn. (3), and the ratio sensitivity is also calculated accordingly. In Fig. 12(a), I_{ON}/I_{OFF} ratio increases as the value of K within the cavity region rises. Reduction in barrier thickness at the tunnelling interface, result in an enhanced electron tunnelling rate. Among all the neutral biomolecules, protein (K=8) biomolecule exhibits large sensitivity in terms of the I_{ON}/I_{OFF} ratio. Moving on to Fig. 12(b), it demonstrates that for DNA biomolecules, both the I_{ON}/I_{OFF} ratio and the I_{ON}/I_{OFF} sensitivity increase with the increment in p, whether it is positive or negative. This is due to the immobilization of a higher value of charge, leading to improved inversion. Consequently, the tunnelling barrier decreases at the source/channel boundary, owing to the development of sudden tunnelling intersection.

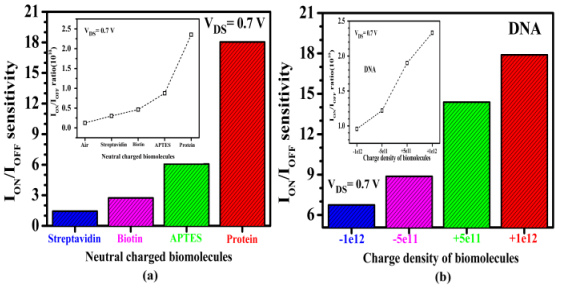

Fig. 12: I_{ON}/I_{OFF} ratio sensitivity graph (a) neutral charge (b) charged (DNA).

V. CONCLUSION

This research introduces a biosensor based on JL-NT-TFET with charge plasma for detecting both neutral and charged biomolecules. By incorporating a nanogap cavity in the inner and outer regions of the JL-NT-TFET, the biosensor's sensing capability is significantly improved. The perpendicular alignment of the nanotube structures facilitates an even dispersal of biomolecules inside the cavity, enhancing detection efficiency. The use of Cr and Ag metals in creating the inner and outer cavities ensures excellent chemical bond and structural strength, providing crucial stability for JL-NT-TFET device. Throughout the study, the sensitivity factor is found to increase in relation between K and p of the biomolecules. However, there is a need to further enhance the sensing ability and introduce new sensing parameters to improve the biosensor's detection speed for various biomolecules, particularly with an initial applied voltage. This approach results in a biosensor with a lower annealing budget, making it more cost-effective and with comparatively higher sensitivity.

REFERENCES

[1] S. Ahish, D. Sharma, Y. B. N. Kumar, and M. H. Vasantha, Performance Enhancement. of Novel InAs/Si Hetero Double-Gate Tunnel FET Using Gaussian Doping, *IEEE Transactions on Electronic Devices*, 63(1), 2016, 288-295.

[2] V. Vijayvargiya, and S. K. Vishvakarma, Effect of drain doping profile on double-gate tunnel field-effect transistor and its influence on device RF performance, *IEEE Transactions on Nanotechnology*, 13(2), 2014, 974-981.

[3] D. Nagy, G. Indalecio, A. J. Garca Loureiro, M. A. Elmessary, K. Kalna, N. Seoane, FinFET versus Gate-All-Around Nanowire FET: Performance, Scaling and Variability, *IEEE Journal of the Electron Devices Society*, 6(1), 2018, 332-340.
[4] J. L. Huguenin, G. Bidal. S. Denorme, D. Fleury, N. Loubet, A. Pouydebasque, and P. Perreau, Gate-all-around technology: taking advantage of ballistic transport, *Solid State Electron*, 9(5), 2010, 883-889.
[5] R. Vishnoi, and M. J. Kumar, A compact analytical model for the drain current of gate-all around nanowire tunnel FET accurate from sub-threshold to ON-state, *IEEE Transactions on Electronic Devices*, 14(1), 2015, 358-362.
[6] H. M. Fahad, and M. M. Hussain, High-performance silicon nanotube tunneling FET for ultralow-power logic applications, *IEEE Transactions on Electronic Devices*, 60(2), 2013, 1034-1039.
[7] A. N. Hanna, and M. M. Hussain, Si/Ge hetero-structure nanotube tunnel field effect transistor, *Journal of Applied. Physics*, 117(1), 2015, 143-150.
[8] B. Ghosh, and M. W. Akram, "Junction less tunnel field effect transistor," *IEEE Electronic Device Letters*, 34(1), 2013, 584-586.
[9] X. Fan, I. M. White, S. I. Shopova, H. Zhu, Jonathan D. Suter and Y. Sun, Sensitive optical biosensors for unlabeled targets: A review, *Scientific Methods*, 6(3), 2018, 826-832.
[10] P. J. Conroy, S. Hearty, P. Leonard, and R. J. O Kennedy, Antibody production, design and use for biosensor-based applications, *Cell and Developmental Biology*, 5(1), 2019, 102-116.
[11] H. Liu, S. Datta, V. Narayanan, Steep switching tunnel FET: A promise to extend the energy efficient roadmap for post-CMOS digital and analog/RF applications, *Low Power Electronics and Design*, 2(1), 2013, 145-150.
[12] K. K. Young, Short-channel effect in fully depleted SOI MOSFETs, *IEEE Transactions on Electronic Devices*, 36(1), 2019, 399-402.
[13] J. P. Colinge, FinFETs and other multi-gate transistors, *IEEE Transactions on Electronic Devices*, 37(1), 2018, 365-374.
[14] R. Hajare, C. Lakshminarayana, G. H. Raghunandan, and C. P. Raj, Performance enhancement of FINFET and CNTFET at different node technologies, *Microsystem Technologies*, 22(1), 2016, 1121-1126.
[15] A. M. Ionescu, and H. Riel, Tunnel field-effect transistors as energy-efficient electronic switches, *Solid State Devices*, 47(9), 2017. 329-337.
[16] S. G. Narendra, Challenges and design choices in nanoscale CMOS, ACM Journal of Emerging Technologies in Computational Systems, 1(5), 2015, 7-49.